# scientific reports

OPEN

# Determination of priority control factors for risk management of heavy metal(loid)s in park dust in Mianyang City

Huaming Du[1,2], Xinwei Lu[2✉] & Xiufeng Han[3]

In order to determine the priority control elements and sources of heavy metal(loid)s (HMs) pollution in park dust, this study collected dust samples from 25 parks in the urban area of Mianyang City and measured the contents of 10 HMs. Based on Monte Carlo simulation, the probabilistic pollution levels and ecological-health risks of HMs were assessed. We found that the average contents of Zn, Co, Pb, and Cr were much higher than their background values in local soil and were influenced by artificial activities. The pollution assessment found that 5 parks were moderately polluted. The comprehensive pollution of HMs in the dust was mainly caused by Zn and Cr, and industrial source was the main contributor to Zn and Cr pollution. The contribution of As, Co, and Pb to the comprehensive ecological risk was high, accounting for 54.6%. Co, Pb, and As were the priority control HMs of ecological risk, while mixed source and industrial source were the priority control sources. HMs presented potential carcinogenic health risks to both children and adults. The non-carcinogenic risk to adults was within safety level, while some parks showed non-carcinogenic risk to children, which should be paid attention to. The source-specific health risk assessment showed that Cr and As were the priority control HMs for human health, while mixed source and industrial source were the priority control sources.

**Keywords** Park dust, Heavy metal(loid), Monte Carlo simulation (MCS), Pollution evaluation, Ecological risk evaluation, Health risk assessment, Priority control factors

The Global Environment Outlook 6 (GEO6) shows that a healthy environment is a prerequisite for economic prosperity, human health, and well-being[1]. With the rapid development of social economy, cities have become the areas most affected by human activities[2,3]. Due to intensive human activities, heavy metal(loid)s (HMs) can accumulate in dust and are difficult to be degraded, making them important environmental indicators and more serious environmental hazards[4]. With the increasing attention to urban environmental quality and human health, HM pollution of dust has gradually become a hot research topic. Researchers have conducted extensive research on the content, sources, pollution assessment, health risks, and environmental effects of HMs in dust[5–9], and have made some progress in studying the distribution characteristics, chemical speciation, particle size effects, sources, and influencing factors of HMs in dust[10–14]. Related studies have shown that urban construction, transportation, and industrial activities have a significant impact on the concentration of HMs in dust. HMs can enter the human body through inhalation, skin contact, and ingestion, posing a threat to human health[15].

Urban parks are important places for city residents to take walks, run, rest, and entertain themselves. Urban park dust is an important carrier of HMs, and the impact of HM pollution in park dust on human health is receiving increasing attention. In recent years, extensive research has been conducted on the pollution of HMs in dust from different urban parks. As reported in the literature[16–22], research has been conducted on the pollution and health risk assessment of HMs in park dust in Trinidad, Krakow, Beijing, Nanjing, Lanzhou, Changchun, and Accra. These studies mainly focused on the content, pollution characteristics, and health risk of HMs in park dust, as well as qualitative source identification using correlation analysis, principal component analysis, and cluster analysis. Quantitative source apportionment using PMF receptor model was rarely conducted. Qualitative source identification can only identify the type of pollution source, cannot provide the contribution rate of the pollution source, and cannot quantify the contribution rate of the pollution source to human health risks. Quantitative apportionment of pollution sources is an important means of scientifically and effectively

[1]School of Resource and Environment Engineering, Mianyang Normal University, Mianyang 621000, China. [2]School of Geography and Tourism, Shaanxi Normal University, Xi'an 710119, China. [3]College of Ecology and Environment, Baotou Teachers' College, Baotou 014000, China. ✉email: luxinwei@snnu.edu.cn

1

controlling environmental pollution. The risk assessment method combining quantitative source analysis with ecological-health risk models can help identify the priority sources for dust HMs pollution control, accurately formulate pollution control measures, reduce management investment, and effectively control the impact of dust pollution on human health. Therefore, the ecological-health risk assessment model of HMs in park dust based on quantitative source analysis has become an important means for scholars to quantitatively identify pollution risks.

The research on HM pollution in park dust in China mainly focuses on large cities[6,19–21], while there is a significant lack of research on HM pollution caused by park dust in emerging industrial cities. Mianyang is a typical emerging industrial city[23], with medicine, new energy, electronic information industry, and auto parts as its main components[24]. In recent years, with the rapid development of industrial production, population increase, urban construction, and urbanization in Mianyang City, the problem of urban ecological environment has become increasingly prominent, and the urban topsoil has been polluted by some HMs[25]. With the intensification of industrial development and urbanization in Mianyang City, the impact of park dust on people's living environment and human health is becoming increasingly significant. However, the pollution status of HMs in park dust and whether there is an exposure risk to citizens urgently need to be addressed. The main purposes of this study were to: (1) measure the concentrations of 10 HMs (Ba, As, Cr, Co, Cu, Pb, Mn, Ni, Zn, and V) in urban park dust of Mianyang using an X-ray fluorescence spectrometer; (2) assess the probabilistic pollution levels, probabilistic ecological risks, and probabilistic human health risk of HMs; and (3) apportion the contribution rates of diverse pollution sources to contamination, ecological, and health risk using the improved Nemerow index (*INI*), Nemerow comprehensive ecological risk index (*NCRI*), and health risk assessment (HRA) model, in order to determine the priority pollution HMs and pollution sources. Our research results aim to offer a scientific basis for the prevention of dust HM contamination and the treatment of priority pollution sources in Mianyang urban parks.

## Sampling and methods
### Study area
The urban area of Mianyang City (104°35'–104°50' E, 31°21'–31°35' N) is situated in the northwest of Sichuan Province. The Fujiang River and Anchang River pass through the city, and the terrain is flat with an average elevation of 490.6 m. The climate of Mianyang urban area is a north subtropical humid monsoon climate. The mean annual temperature is 16.6 °C, and the average annual precipitation is 878.2 mm[26]. The study area is mainly composed of fluvial alluvium, sandstone, and mudstone weathering material. The main urban area of Mianyang includes most of the industrial, commercial, and residential areas. By the end of 2022, the built-up area of Mianyang city had reached 189.2 km$^2$, the urban industrial land area had reached 34.9 km$^2$, and the urban resident population had reached 2.3 million[27]. The ecological environment of Mianyang city is facing severe challenges brought by rapid urbanization and industrialization[25,26].

### Dust sampling and experimental analysis
After field investigation, we selected the gate entrances, sidewalks, entertainment areas, and sports field of each park as sampling points, collected dust with plastic brush and dustpan, and mixed the collected dust from each park into one sample. From January to February 2022, a total of 25 mixed dust samples were collected in the parks of Mianyang urban area (Fig. 1). For each sample, after removing the plant residue and bricks from the dust[26], the mixed dust samples of 200 g were stored in a polyethylene bag with a sample label on it. Finally, the surrounding environmental conditions at the time of sample collection were recorded.

The samples were placed indoors and air-dried under natural conditions. After grinding with agate mortar, passed through a 20 mesh nylon sieve, then ground with vibration grinder and passed through a 200 mesh nylon screen, finally the ground dust samples were sealed in polyethylene self-sealing bags for testing[28]. The 5.0 g sample of ground dust was pressed into circular sheets by a press machine, and the concentrations of Ba, As, Cr, Co, Cu, Ni, Pb, Mn, V, and Zn in the samples were measured by X-ray fluorescence spectrometer (XRF, Bruker, S8 Tiger, Germany)[29]. To ensure the accuracy of the measurement results, the instrument components were cleaned and debugged before analysis. Our quality control was carried out with 10% duplicate samples[28] and soil standard material (GSS-3), with an analysis error within 5%.

### Geo-accumulation index (*I*$_{geo}$) and improved Nemerow index (*INI*)
The *I*$_{geo}$ is used to evaluate the contamination degree of a single HM, and it is calculated using the following Eq. (1)[30]:

$$I_{geo} = \log_2 \frac{C_i}{1.5 \cdot B_i} \tag{1}$$

where $C_i$ is the content of HM $i$ in park dust, mg kg$^{-1}$; $B_i$ is the geochemical reference value of HM $i$, mg kg$^{-1}$.

*INI* is applied to evaluate the comprehensive contamination degree of all HMs, and it is calculated using the following Eq. (2)[31]:

$$INI = \sqrt{\frac{I_{geo}\max^2 + I_{geo_{avg}}^2}{2}} \tag{2}$$

where $I_{geo}\max$ and $I_{geo_{avg}}$ represent the maximum and average $I_{geo}$ values of the evaluated HMs, respectively. The pollution degree of $I_{geo}$ and *INI* are shown in Table S1.
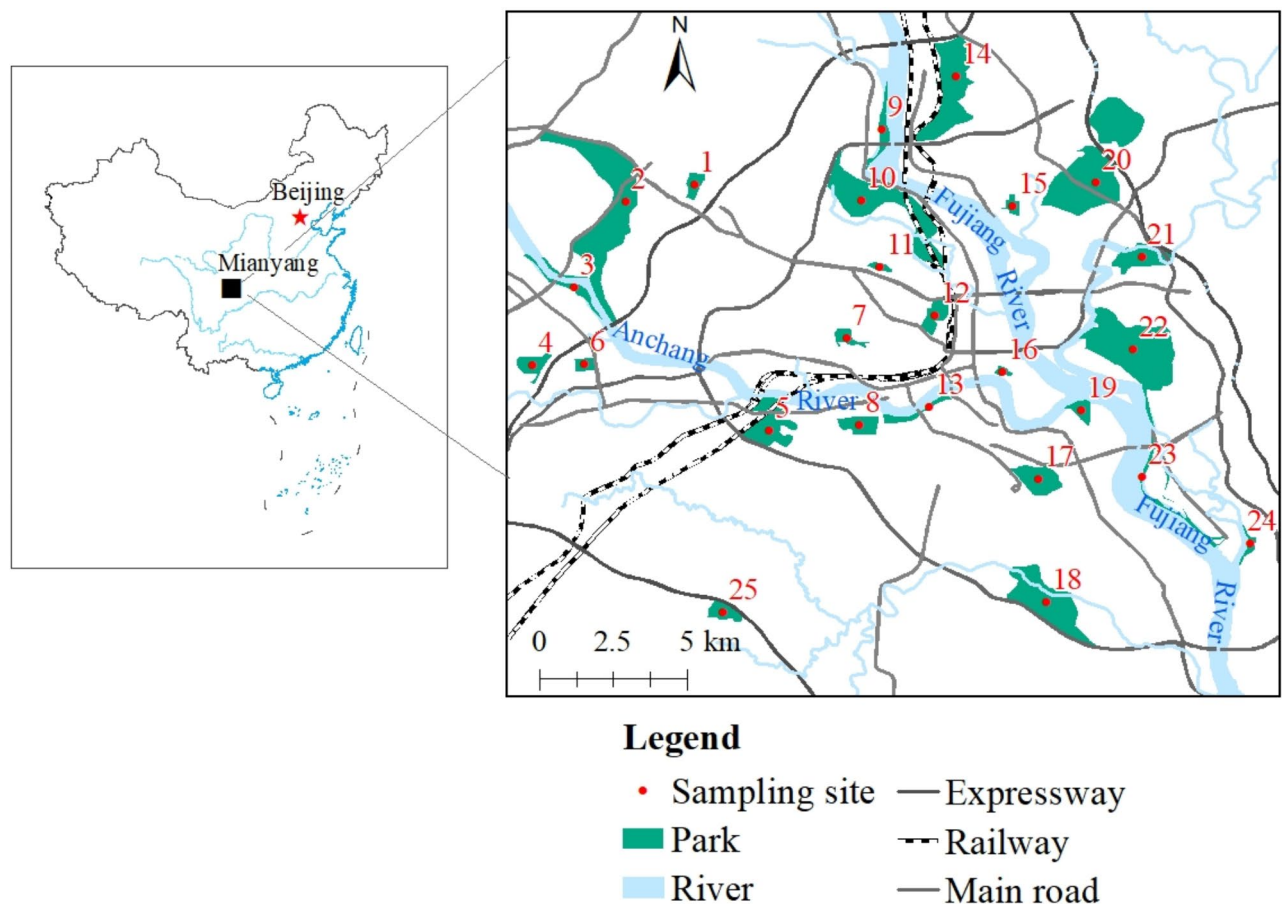
**Fig. 1**. Park dust sampling points of Mianyang urban area [the figure was generated by Huaming Du using the ArcGIS 10.3 (https://developers.arcgis.com/)].

### The potential ecological risk factor ($E_i$) and the Nemerow comprehensive ecological risk index (*NCRI*)

$E_i$ is used to assess the ecological risk of a single HM, and it is calculated using the following Eq. (3)[32]:

$$E_i = T_i \times \frac{C_i}{B_i} \tag{3}$$

where $T_i$ is the toxicity coefficient of HM *i*. The toxicity coefficients of Ba, Mn, Zn, Cr, V, Pb, Cu, Co, Ni, and As are 1, 1, 1, 2, 2, 5, 5, 5, 5, 10, respectively[31].

*NCRI* is mainly used to assess the comprehensive ecological risk of all HMs in dust, and it is calculated by Eq. (4)[31]:

$$NCRI = \sqrt{\frac{E_{i\max}^2 + E_{i_{avg}}^2}{2}} \tag{4}$$

where *NCRI* is the Nemerow comprehensive ecological risk index of all HMs in dust. $E_{i\max}$ and $E_{i_{avg}}$ represent the maximum and average $E_i$ values of the evaluated HMs, respectively. Table S2 shows the grade of $E_i$ and *NCRI*.

### Health risk assessment model (HRA) of HMs

The health risk assessment of HMs in park dust was based upon the USEPA human risk assessment model. All of the 10 HMs detected have chronic non-carcinogenic risks, As, Cr, Ni, and Co also have carcinogenic risks[13,31]. The exposure dose is calculated by Eqs. (5)–(7)[31–37]:

$$ADI_{ing} = \frac{C \times IR_{ing} \times EF \times ED}{BW \times AT} \times 10^{-6} \tag{5}$$

$$ADI_{inh} = \frac{C \times EF \times IR_{inh} \times ED}{PEF \times BW \times AT} \tag{6}$$

$$ADI_{dermal} = \frac{C \times SA \times SL \times ABS \times EF \times ED}{BW \times AT} \times 10^{-6} \tag{7}$$

where $ADI_{ing}$, $ADI_{inh}$, and $ADI_{dermal}$, respectively, represent the average daily exposure dose (mg kg$^{-1}$ day$^{-1}$) via direct ingestion, inhalation, and dermal absorption; $C$ is the concentration (mg kg$^{-1}$) of HMs (95% UCL), mg kg$^{-1}$; $IR_{ing}$ is the ingestion rate, mg day$^{-1}$; $EF$ refers to exposure frequency, day year$^{-1}$; $ED$ means exposure time, year; $BW$ means average body weight, kg; $AT$ is the average time, day; $IR_{inh}$ means inhalation rate, m$^3$ day$^{-1}$; $PEF$ is the particle emission factor, m$^3$ kg$^{-1}$; $SA$ is exposed skin area, cm$^2$; $SL$ is skin adhesion factor, mg cm$^{-2}$ day$^{-1}$; $ABS$ means dermal absorption factor. Table S3 shows the meanings and values of all parameters[38–42].

The total non-carcinogenic risk index ($HI$) and the total carcinogenic risks ($TCR$) of all HMs in park dust are calculated by Eq. (8) and Eq. (9), respectively[43–46]:

$$HI = \sum HQ_i = \sum \frac{ADI_{ij}}{RfD_{ij}} \tag{8}$$

$$TCR = \sum CR_i = \sum (ADI_{ij} \times SF_{ij}) \tag{9}$$

Where $HQ_i$ and $CR_i$ are the non-carcinogenic risk and carcinogenic risk values of a single HM $i$, respectively; $RfD_{ij}$ is the reference dose (Table S4), $SF_{ij}$ is the carcinogenic slope factor (Table S4). The risk levels for $HI$ and $TCR$ are shown in Table S5.

## Monte Carlo simulation (MCS)

In order to accurately reflect the risk characteristics of HMs in park dust, MCS was used to evaluate the risk probability of HMs based on the uncertainty of HM content in this study[47], and at the same time, the contribution of each HM to the risk was quantitatively evaluated, and the main risk contributing factors were identified. The principle of this method was to sample repeatedly from the probability distribution of several input variables to obtain the distribution of the output variables. In this study, the contents of 10 HMs in park dust are taken as the uncertain parameter, and the distribution characteristics of the 10 HMs are shown in Table 1. We set $I_{geo}$, $INI$, $E_i$, $NCRI$, $HI$, and $TCR$ as target variables, and then simulated the pollution level, ecological risk, and human health risk of HMs in park dust 10,000 times using Crystal Ball software based on Eqs. (1), (2), (3), (4), (8), and (9), respectively.

## Results and discussion
### Contents of HMs in dust

The HM content in park dust of the study area and the background values of the topsoil in Sichuan Province are shown in Table 2. The contents of As, Ba, Co, Cr, Cu, Mn, Ni, Pb, Zn, and V in park dust ranged from 5.0 to 16.3, 399.5–1084.5, 7.8–67.1, 60.9–378.3, 23.3–61.1, 411.2–975.6, 18.2–41.6, 21.2–211.3, 75.7–306.3, and 52.5–93.1 mg kg$^{-1}$, respectively. Table 2 shows that the mean contents of Ba, Cr, Co, Pb, Zn, and Cu were 1.4, 2.3, 1.9, 1.7, 2.1, and 1.2 times of their background values[48], respectively. The coefficient of variation (CV) of HMs is used to study the variation and dispersion of HMs in regional sampling sites. When the CV of the HM content in the study area is greater than 20%, it is considered to be disturbed by human activities[29]. Table 2 shows that the CV values of Pb (80.9%), Co (66.0%), and Cr (55.2%) in park dust were much higher than 20%, indicating that Pb, Co, and Cr were greatly influenced by human activities. The CV values of Ba (23.7%) and Mn (20.3%) were close to the critical values, indicating that human activities had some affection on the distribution of these 2 HMs in park dust. However, Ni (19.7%) and V (15.2%) with small CV values might be mainly influenced by natural factors.

Comparing the concentration of HMs in park dust of Mianyang City with that in 12 urban parks in China (Table 2), the concentration of As in park dust of Mianyang City was lower than that in Nanjing, Lanzhou, Wuhan, Zhengzhou, and Jiaozuo, but higher than that in Baotou. The concentration of Ba was slightly higher than that in Baotou. The concentration of Cr was higher than that in Beijing, Nanjing, Lanzhou, Changchun, Wuhan, Zhengzhou, Chengdu, Xi'an, Hangzhou, Baotou, and Jiaozuo. The content of Co was lower than that in

| Element | Mean | Median | Standard deviation | Minimum | Maximum | Distribution |
|---|---|---|---|---|---|---|
| As | 7.3 | 6.8 | 2.3 | 5 | 16.3 | Lognormal |
| Ba | 662.1 | 652.2 | 157.2 | 399.5 | 1084.5 | Logistic |
| Cr | 178.7 | 180.5 | 98.6 | 60.9 | 378.3 | Beta |
| Co | 33.7 | 35.2 | 22.2 | 7.8 | 67.1 | Beta |
| Cu | 38.7 | 35.9 | 10.1 | 23.3 | 61.1 | Lognormal |
| Ni | 26.0 | 24.5 | 5.1 | 18.2 | 41.6 | Max Extreme |
| Pb | 51.0 | 42.3 | 41.2 | 21.2 | 211.3 | Lognormal |
| Mn | 646.7 | 651.3 | 131.6 | 411.2 | 975.6 | Beta |
| Zn | 185.0 | 195.4 | 57.2 | 75.7 | 306.3 | Beta |
| V | 66.7 | 63.7 | 10.1 | 52.5 | 93.1 | Lognormal |

**Table 1.** Distribution test and fitting results of HM contents.

| Element | As | Ba | Cr | Co | Cu | Ni | Pb | Mn | Zn | V |
|---|---|---|---|---|---|---|---|---|---|---|
| Minimum | 5.0 | 399.5 | 60.9 | 7.8 | 23.3 | 18.2 | 21.2 | 411.2 | 75.7 | 52.5 |
| Maximum | 16.3 | 1084.5 | 378.3 | 67.1 | 61.1 | 41.6 | 211.3 | 975.6 | 306.3 | 93.1 |
| Mean | 7.3 | 662.1 | 178.7 | 33.7 | 38.7 | 26.0 | 51.0 | 646.7 | 185.0 | 66.7 |
| Standard deviation | 2.3 | 157.2 | 98.6 | 22.2 | 10.1 | 5.1 | 41.2 | 131.6 | 57.2 | 10.1 |
| Coefficient of variation (%) | 31.5 | 23.7 | 55.2 | 66.0 | 26.0 | 19.7 | 80.9 | 20.3 | 30.9 | 15.2 |
| Reference value[48] | 10.4 | 474.0 | 79.0 | 17.6 | 31.1 | 32.6 | 30.9 | 657.0 | 86.5 | 96.0 |
| Beijing[18] | NA | NA | 69.3 | NA | 72.1 | 26.0 | 201.8 | NA | 219.2 | NA |
| Nanjing[19] | 17.3 | NA | 133.0 | 11.5 | 141.0 | 115.0 | 119.0 | 602.0 | 585.0 | 43.3 |
| Lanzhou[20] | 12.3 | NA | 78.8 | NA | 54.3 | 36.2 | 65.8 | NA | 246.5 | NA |
| Changchun[21] | NA | NA | 59.3 | NA | 37.8 | 23.1 | 69.1 | NA | 169.3 | NA |
| Wuhan[9] | 10.3 | NA | 72.0 | NA | 47.4 | 28.2 | 45.8 | 682.1 | 184.2 | NA |
| Zhengzhou[49] | 12.1 | NA | 34.8 | NA | 16.0 | 11.7 | 34.4 | NA | 94.2 | NA |
| Chengdu[50] | NA | NA | 55.3 | NA | 61.0 | 20.1 | 78.8 | NA | 275.0 | NA |
| Hong Kong[51] | NA | NA | NA | NA | 138.8 | NA | 248.1 | 496.8 | 1998.0 | NA |
| Xi'an[52] | NA | NA | 153.4 | 35.6 | 36.4 | 26.8 | 78.0 | 330.5 | 91.2 | 54.0 |
| Hangzhou[53] | NA | NA | 54.0 | 22.0 | 69.0 | 28.9 | 95.4 | 536.0 | 194.8 | NA |
| Baotou[8] | 6.5 | 640.4 | 154.1 | 52.9 | 26.9 | 25.1 | 36.2 | 504.4 | 49.7 | 71.3 |
| Jiaozuo[13] | 23.1 | NA | 112.1 | 25.3 | 49.9 | 51.7 | 55.3 | 473.8 | 374.3 | NA |

**Table 2**. The contents (mg kg$^{-1}$) of HMs in Mianyang park dust and other published park dust in China. NA means not available.

Baotou and Xi'an, but higher than that in Jiaozuo, Hangzhou, and Nanjing. The concentration of Cu was lower than that in Beijing, Nanjing, Lanzhou, Wuhan, Chengdu, Hong Kong, Hangzhou, and Jiaozuo, but higher than that in Changchun, Zhengzhou, Xi'an, and Baotou. The content of Ni was similar to Beijing, lower than that in Nanjing, Lanzhou, Wuhan, Xi'an, Hangzhou, and Jiaozuo, and higher than that in Changchun, Zhengzhou, Chengdu, and Baotou. The concentration of Pb was lower than that in Beijing, Nanjing, Lanzhou, Changchun, Chengdu, Hong Kong, Xi'an, Hangzhou, and Jiaozuo, but higher than that in Wuhan, Zhengzhou, and Baotou. The concentration of Mn was lower than that in Wuhan, but higher than that in Nanjing, Hong Kong, Xi'an, Hangzhou, Jiaozuo, and Baotou. The content of Zn was lower than that in Beijing, Nanjing, Lanzhou, Chengdu, Hong Kong, Hangzhou, and Jiaozuo, but higher than that in Changchun, Wuhan, Zhengzhou, Xi'an, and Baotou. The content of V was lower than that in Baotou, but higher than that in Xi'an and Nanjing. Compared with other 12 cities, we found that the concentrations of Ba, Mn, and Cr in park dust of Mianyang urban zone were slightly higher, the contents of Co and V were at a moderate level, and the concentrations of As, Pb, Cu, Zn, and Ni were slightly lower. The contents of HMs in urban park dust is closely related to the regional geological environment, urban scale, industrial activities, urban traffic, and people's environmental protection awareness. The specific reasons need further investigation and analysis.

### Results of contamination evaluation based on MCS
Table S6 shows the results of the geo-accumulation assessment of HMs in urban park dust, and we found that the simulated mean $I_{geo}$ values of all HMs were consistent with the detected mean $I_{geo}$ values. The mean $I_{geo}$ values of HMs in park dust were Zn > Cr > Co > Pb > Ba > Cu > Mn > Ni > V > As. The average $I_{geo}$ values of Zn and Cr were between 0 and 1, indicating that the pollution degree of Zn and Cr was unpolluted to moderately polluted. However, the $I_{geo}$ values of Zn in park 22 and the $I_{geo}$ values of Cr in park 5, 8, 10, 12, 17, 19, 22, and 24 were all greater than 1, indicating moderate pollution (Figure S1). The average $I_{geo}$ values of Co, Pb, Ba, Cu, Mn, Ni, V, and As were all less than 0, which were − 0.1, -0.1, -0.1, -0.3, -0.6, -0.9, -1.1, and − 1.2, respectively, indicating that these HMs were generally unpolluted. However, it was worth noting that the $I_{geo}$ values of As in park 22, Ba in park 6, 8, 10, 12, 13, 22, and 25, Cu in park 6, 8, 11, 16, and 24, were all greater than 0, indicating non-pollution to moderate pollution (Figure S1). In 7 parks, Co was unpolluted to moderately polluted, while in 7 parks is presented moderate pollution. Regarding Pb, 5 parks were unpolluted to moderately unpolluted, 2 parks were moderately unpolluted, and 1 park was moderately to heavily unpolluted. Overall, the HM contamination degree in park dust of the study area was relatively low.

The simulated $INI$ values of HMs at every park were basically consistent with the detected $INI$ values (Table S7). In addition, the sensitivity analysis showed that the sensitivity of Zn and Cr were 50.0% and 29.0% (Figure S2), respectively, indicating that the comprehensive contamination of HMs in dust of Mianyang urban parks was mainly caused by Zn and Cr. The comprehensive contamination levels of HMs at each park are shown in Fig. 2. Figure 2 showed that most of parks were unpolluted to moderately polluted, while park 5, 15, 21, 22, and 24 were moderately polluted.

According to our previous source appointment results[26], the source-oriented pollution assessment indicated that industrial source was the main contributor to Zn and Cr pollution (Fig. 3a). HMs from building sources, mixed sources, and industrial sources exhibited uncontaminated to moderately contaminated, while HMs from natural sources presented moderately contaminated (Fig. 3b). Overall, anthropogenic industrial sources

contribute significantly to HM pollution in park dust, which is related to the pollutant emissions caused by the rapid development of industry in Mianyang[27].

## Results of ecological risk evaluation based on MCS

The simulated mean $E_i$ values and detected mean $E_i$ values of HMs in Mianyang urban park dust were basically the same (Table S8). The mean $E_i$ values of 10 HMs in park dust were as follows: Co > Pb > As > Cu > Cr > Ni > Zn > Ba > V > Mn. Overall, the mean $E_i$ values of all HMs belong to low risk. Figure S3 showed that the $E_i$ values of Ba, Cr, Cu, Ni, Mn, Zn, and V in park dust were less than 15, presenting low risk. The mean $E_i$ value of Co was the highest, and 7 parks were moderate risk. Next is Pb, park 15 and 25 were moderate risk and park 22 exhibited considerable risk. In addition, park 22 presented moderate risk of As.

The simulated NCRI values of HMs at each park were close to the detected values (Table S9). Figure 4 shows the spatial distribution of the NCRI values of HMs in all parks. From Fig. 4, it can be seen that in 23 parks had NCRI values < 15, indicating low risk. 2 parks had NCRI values between 15 and 30, indicating moderate risk. The moderate risk samples are mainly distributed in industrial zones in the east. Based on the sensitivity analysis of NCRI predictions value (Figure S4), it was found that Pb, As, Cu, Ni, and Co played a dominant role in NCRI, and their sensitivities were 33.3%, 24.0%, 18.1%, 11.3%, and 7.2%, respectively. This may be related to the toxicity coefficients of diverse HMs. The toxicity coefficients of Pb, As, Cu, Ni, and Co were 5, 10, 5, 5, and 5, respectively, which were higher than those of other HMs. The key to controlling the ecological risk was to reduce the concentrations of Pb, As, Cu, Ni, and Co in park dust.

The results (Fig. 5) of source-oriented NCRI assessment indicated that the contribution rates of the four sources of HMs in park dust to the comprehensive ecological risk in the study area, from high to low, were as follows: mixed source of natural and traffic (33.6%) > industrial source (28.3%) > building source (21.0%) > natural source (17.1%), with the mixed source having the highest impact on ecological risk. From the analysis of the contribution value of HMs from diverse pollution origins to the comprehensive ecological risk, the total risk of Co and Pb accounted for more than 39.2%, indicating that Co and Pb were the chief contributing HMs to the ecological risk. In addition, the toxicity coefficient of As was much higher than those of other HMs, so it had a high ecological risk, with a contribution rate of 15.4% to ecological risk. In summary, As, Pb, and Co were the preferred HMs for dust ecological risk control in the study area, while mixed source and industrial source were the priority sources.

By comparing the results of $I_{geo}$, INI, $E_i$, and NCRI, we found that due to the different focus of these evaluation methods, the result of $I_{geo}$ and INI were slightly different from those of $E_i$ and NCRI. $I_{geo}$ and INI mainly consider the geochemistry factors, focusing on the influence of dust HM contents and their background values, with an emphasis on the human impact of HMs. Besides the contents of HMs, $E_i$ and NCRI also take into account the toxicity difference of different HMs, so more attention should be paid to the contamination prevention and control of HMs with obviously higher toxicity coefficients such as As and Pb. The combination of these assessment methods can objectively and comprehensively reflect the current status of HM contamination in park dust, providing a basis for future environmental protection and pollution control.

## HRA of HMs based on MCS

The simulated and detected exposure doses of HMs by different routes were basically consistent (Table S10). From the exposure paths of HMs, we found that both non-carcinogenic and carcinogenic daily exposure doses for adults and children followed the pattern of $ADI_{ing} > ADI_{dermal} > ADI_{inh}$, indicating that direct ingestion was
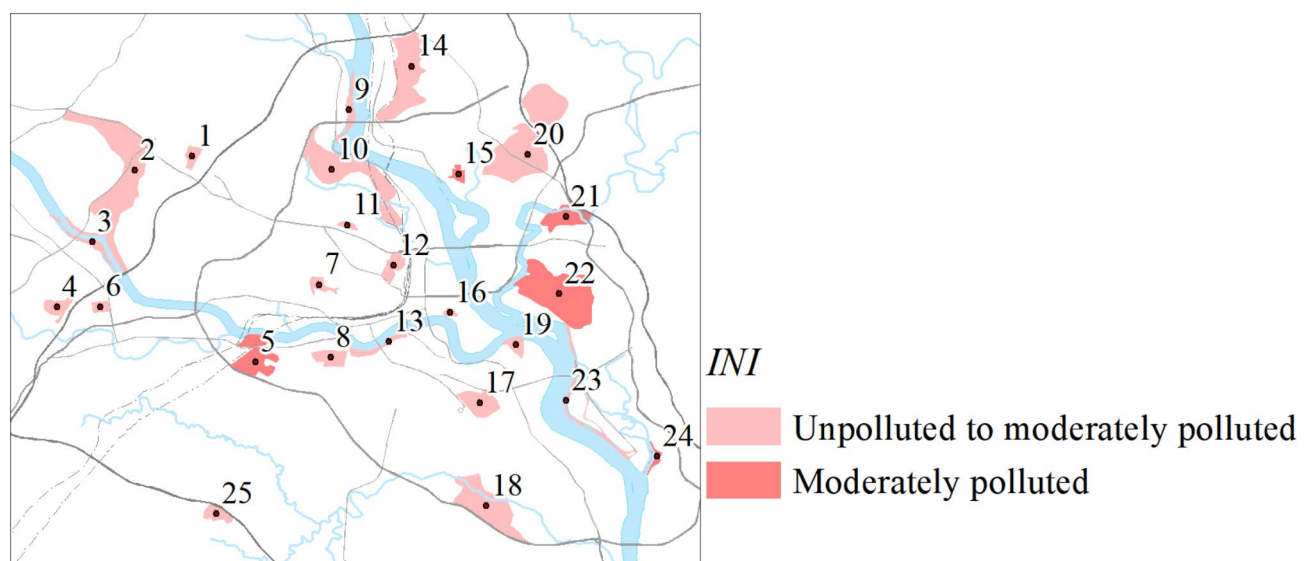


**Fig. 2**. The INI degree of HMs in Mianyang urban park dust [the figure was generated by Huaming Du using the ArcGIS 10.3 (https://developers.arcgis.com/)].
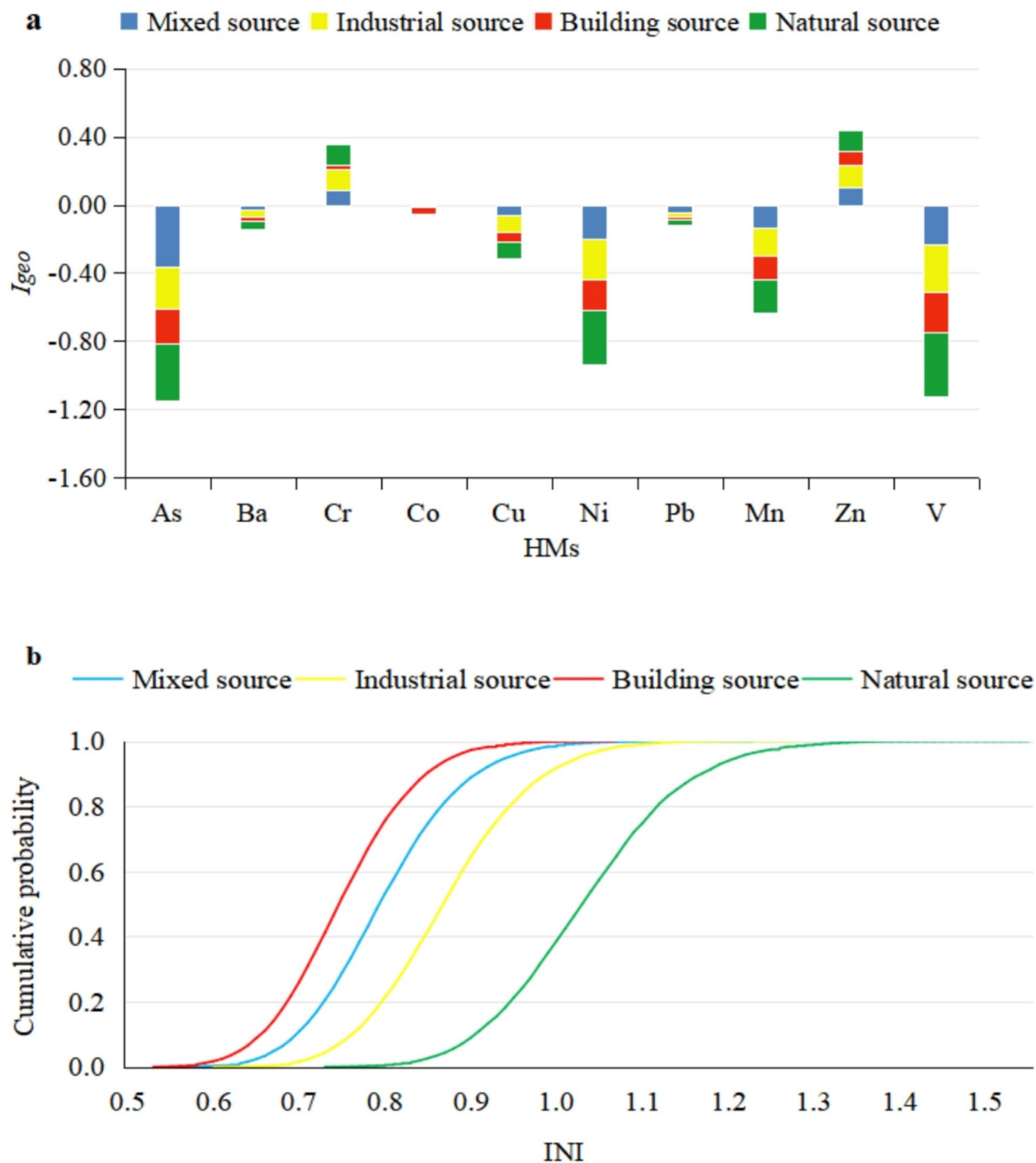
**Fig. 3**. The source-specific probabilistic contamination level of HMs in park dust [the figure was generated by Huaming Du using the ArcGIS 10.3 (https://developers.arcgis.com/)].

the primary way of exposure risk of HMs in park dust, accounting for over 89% of the total daily exposure dose. From the perspective of the population, the exposure dose of children was much greater than that of adults, which may be due to their frequent hand-mouth behavior and higher inhalation rate per unit weight, resulting in children being more exposure to and ingestion of HM-contaminated dust particles than adults.

The concentrations of 10 HMs were taken as the uncertainty parameter, probability ranges and sensitivity analyses (Figures S5 and S6) of non-carcinogenic and carcinogenic risks for children and adults were obtained
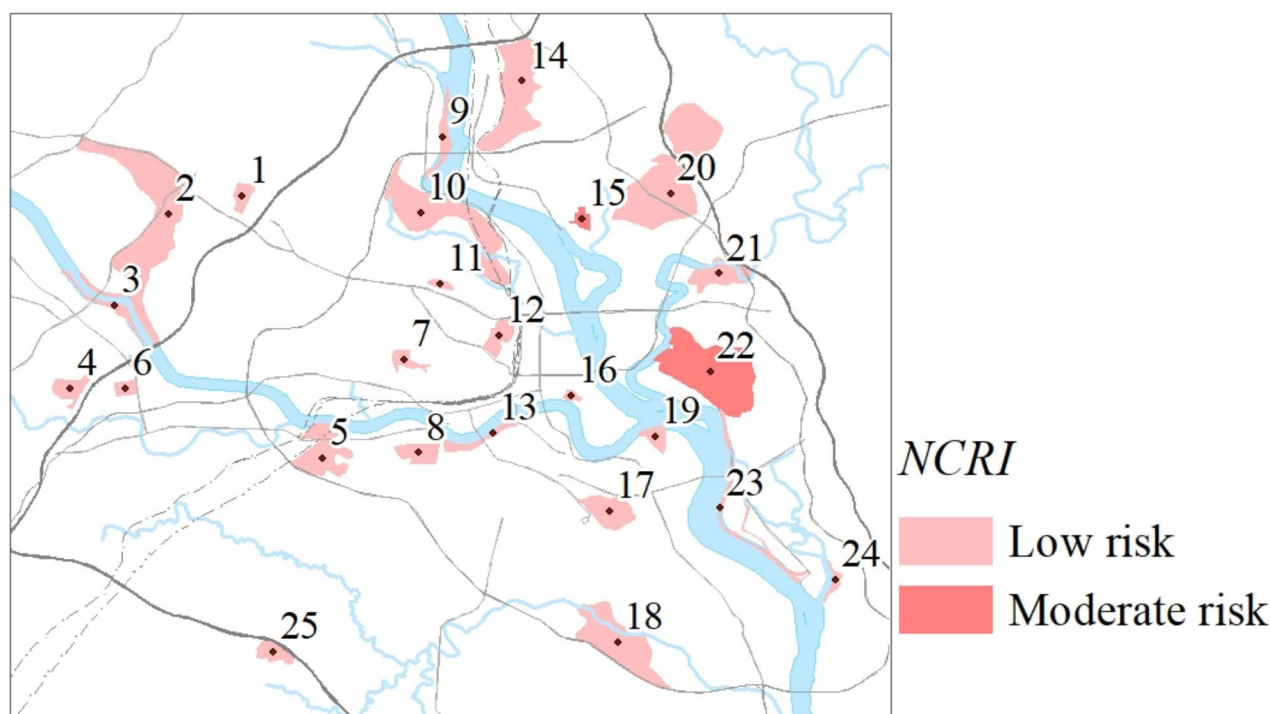
**Fig. 4**. The *NCRI* level of HMs in park dust [the figure was generated by Huaming Du using the ArcGIS 10.3 (https://developers.arcgis.com/)].

using Crystal Ball software after 10,000 simulations[54]. The simulated *HI* values and *TCR* values were consistent with the detected *HI* values and *TCR* values for both children and adults (Table S11).

The simulated average *HI* values for children and adults were 7.7E-01 and 1.3E-01, respectively, both less than the USEPA guideline value of 1, indicating the non-carcinogenic risk was minimal or negligible. The value of the 5th percentile is generally considered the least harmful, while the value of the 95th percentile is considered the worst-case scenario[47]. The 95% confidence level of non-carcinogenic risk in children was (7.3E-01, 8.1E-01), and the 95% confidence level of non-carcinogenic risk in adults was (1.2E-01, 1.4E-01). The 95% *HI* for children and adults were all lower than 1, indicating that HMs do not pose a non-carcinogenic risk to human health. Table S11 shows that the order of non-carcinogenic risks of 10 HMs in park dust to adults and children was as follows: $Cr > As > Mn > Pb > V > Ba > Co > Ni > Cu > Zn$, and the non-carcinogenic risk of each HM was lower than 1, indicating that the non-carcinogenic risk caused by HMs from all sources was at a safe level. However, the *HI* value of children was 0.8, which is close to the critical value of non-carcinogenic risk (1), indicating that the HMs in park dust have potential non-carcinogenic risks to children. The non-carcinogenic risks of direct ingestion by children through hand-mouth cannot be ignored and should be taken seriously.

The carcinogenic risk order of Ni, Cr, Co, and As in dust for children and adults was $As > Cr > Co > Ni$. Table S11 showed that the simulated average *TCR* values of children and adults were $5.3 \times 10^{-6}$ and $3.7 \times 10^{-6}$, respectively. The 95% confidence levels for carcinogenic risk in children were (4.2E-06, 6.7E-06) and in adults were (2.9E-06, 4.7E-06), showing that the 4 HMs have potential carcinogenic risk to children and adults. Combining content and pollution evaluation, it was found that although the content of As in dust was low and the pollution degree was not high, its carcinogenic risk cannot be ignored.

Figure 6 showed that the non-carcinogenic risks for children in parks 5, 15, 22, and 24 were all higher than 1, indicating that these parks had obvious non-carcinogenic risk for children. The non-carcinogenic risk values for children in parks 4, 8, 10, 12, 17, 19, and 25 (0.8–1.0) were close to the critical value of non-carcinogenic risk, and showed a larger trend of non-carcinogenic risk to children. The non-carcinogenic risks to adults were negligible in all parks. The *TCR* values of children and adults were all greater than $10^{-6}$, indicating a potential carcinogenic risk in all parks, which should be taken seriously.

Through the sensitivity analysis of non-carcinogenic risk, it was found that As, Cr, Ba, V, and Pb had significant effects on the non-carcinogenic risk for both children and adults. The contribution rates of As and Cr to the non-carcinogenic risk in children were 36.6% and 34.6%, respectively, and the contribution rates of As and Cr to the non-carcinogenic risk in adults was 35.5% and 32.8%, respectively (Figure S5), indicating that As and Cr had a significant impact on non-carcinogenic risks in children and adults. The result of carcinogenic risk sensitivity is shown in Figure S6. As had the highest sensitivity and should be regarded as the priority control element, followed by Cr. The sensitivity of $IR_{ing}$ to children and adults was 5.4% and 1.1%, respectively, indicating that reducing direct intake can greatly reduce the carcinogenic risk.

Health risk assessment can only help understand the level of risk, but cannot effectively control health risks. Therefore, it is need to screen the priority control HMs in dust pollution control and identify key pollution
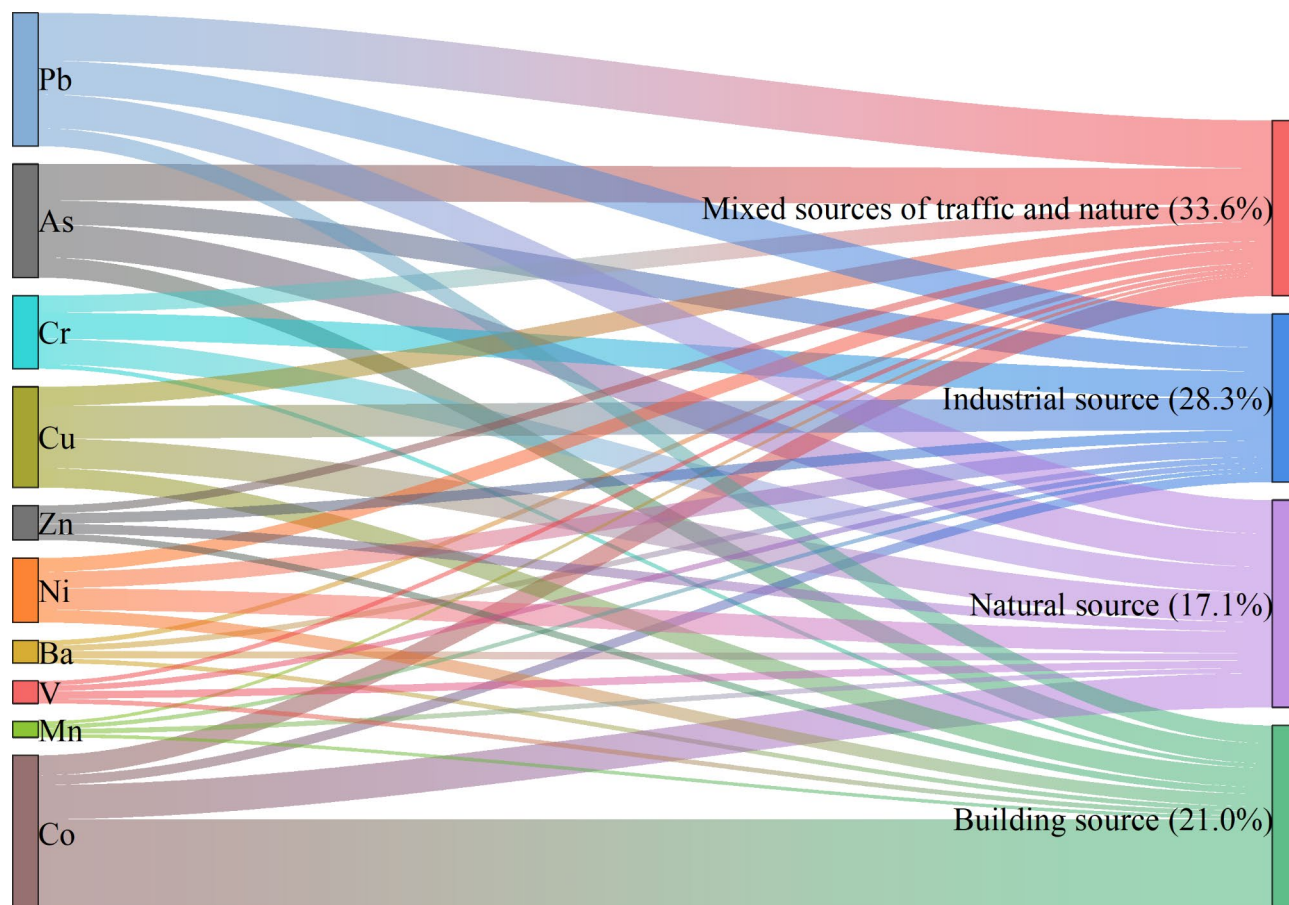
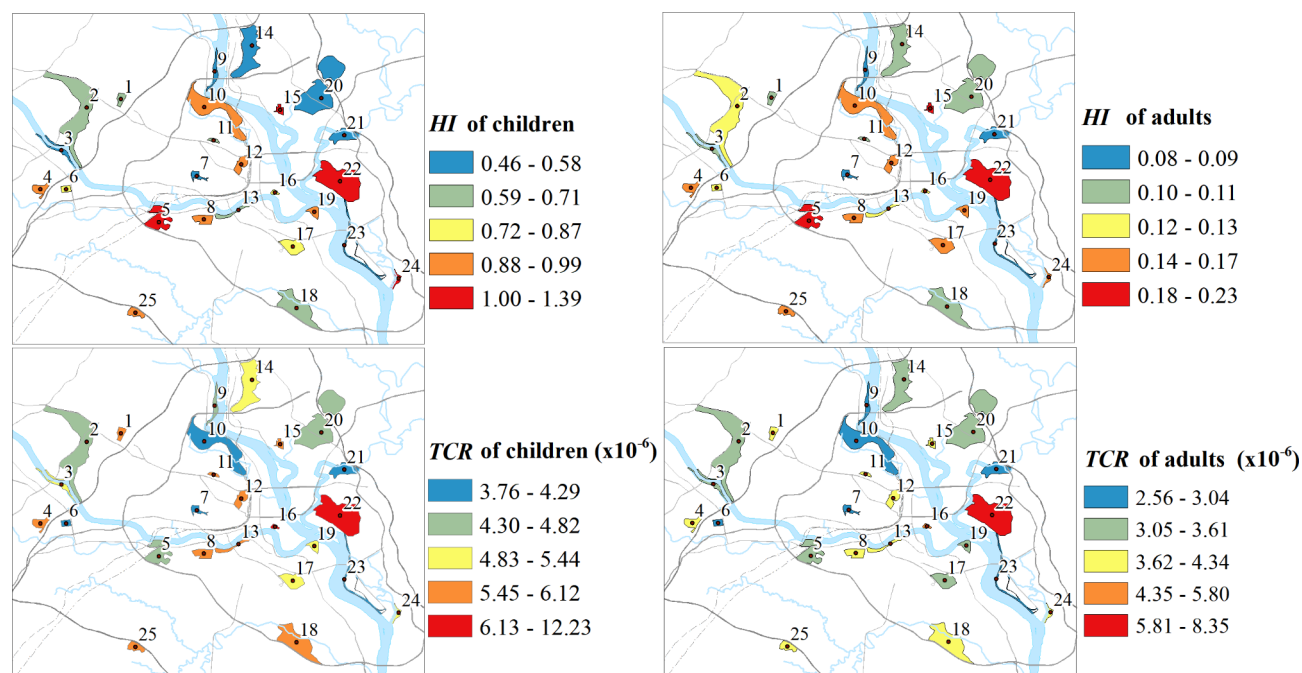**Fig. 5**. Contribution rate of HMs in diverse sources to comprehensive ecological risk.



**Fig. 6**. Distribution of *HI* and *TCR* in different parks [the figure was generated by Huaming Du using the ArcGIS 10.3 (https://developers.arcgis.com/)].
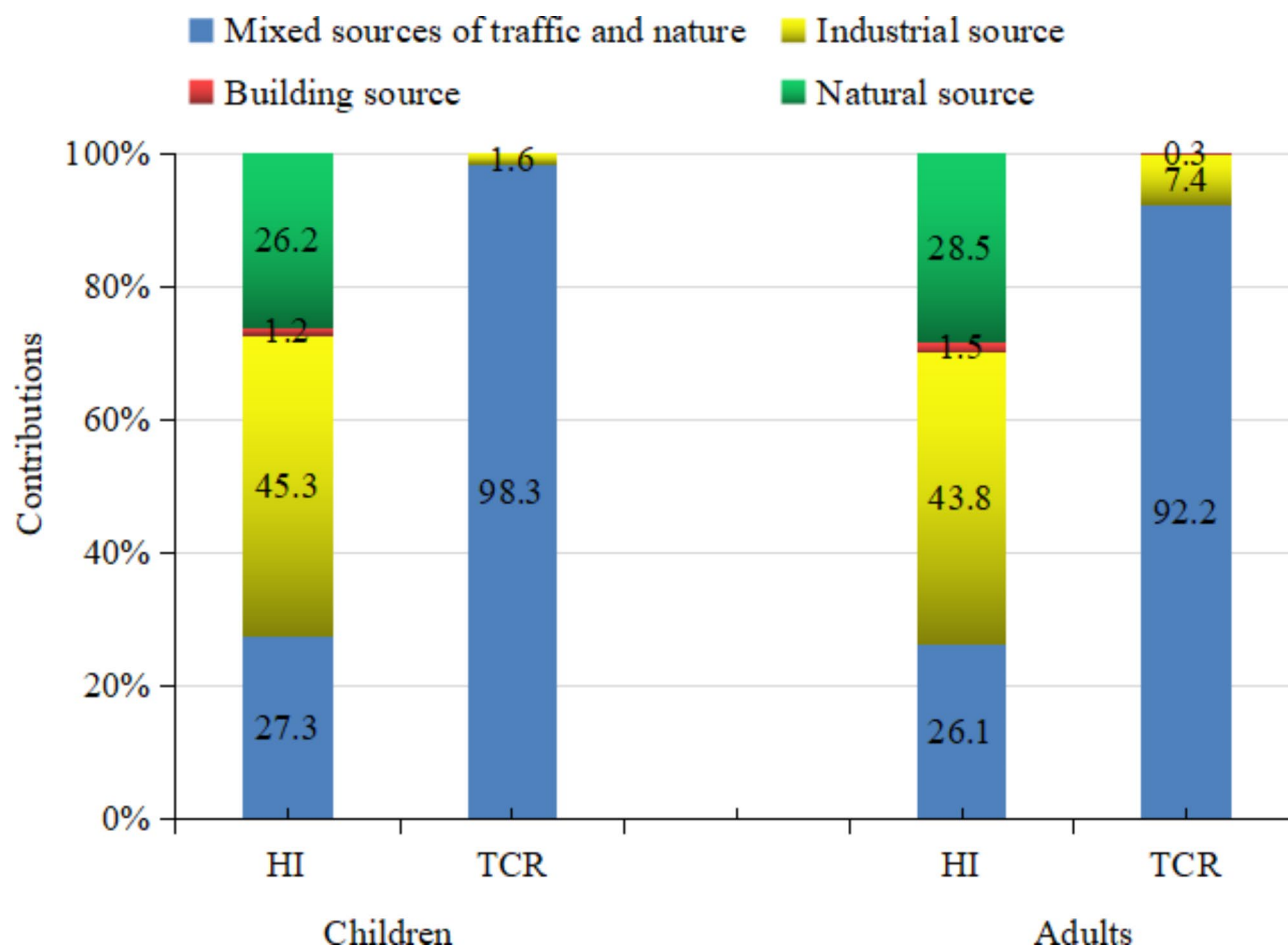
**Fig. 7**. Contribution rates of diverse pollution origins to non-carcinogenic risks and carcinogenic risks of children and adults.

sources. In this study, we assessed non-carcinogenic and carcinogenic risks of HMs from different sources, as shown in Fig. 7. Industrial source contributed the most to non-carcinogenic risks for children and adults. The contribution rates of the 4 sources to carcinogenic risk for children and adults were mixed sources > industrial source > building source > natural source.

## Conclusion

The concentrations of Cr, Zn, Co, and Pb in park dust were significantly higher than their background values, which were 2.3, 2.1, 1.9, and 1.7 times higher than their background values, respectively. The accumulation of Zn and Cr is most evident in dust. Zn in 1 park and Cr in 9 parks were moderately polluted, with industrial source being the main source of Zn and Cr pollution. The ecological risks of As, Co, and Pb were higher than those of other HMs. Mixed source and industrial source contribute the most to ecological risks and are the priority control sources. Co, Pb, and As are the priority control sources for ecological risks. The non-carcinogenic risks caused by HMs in park dust are within an acceptable range for adults, while 4 parks had non-carcinogenic risks for children. There has a potential carcinogenic risk for both children and adults in all parks. Overall, children in the study area had higher non-carcinogenic and carcinogenic health risks compared to adults. Industrial and mixed sources are the priority control sources for health risks, while As and Cr are the priority HMs.

## Data availability

The datasets used and/or analyzed during the current study are available from the corresponding author on reasonable request.

## References

1. UNEP (United Nations Environment Programme). *Global Environment Outlook 6: Healthy Planet, Healthy People*. Sep (2023). https://www.unep.org/resources/assessment/global-environment-outlook-6-other-language-versions. Accessed 12.

2. Aguilera, A. et al. Heavy metal pollution of street dust in the largest city of Mexico, sources and health risk assessment. *Environ. Monit. Assess.* **193**, 193. https://doi.org/10.1007/s10661-021-08993-4 (2021).

3. Haghnazar, H., Soltani-Gerdefaramarzi, S., Ghasemi, M. & Johannesson, K. H. Receptor model-based approach to estimate urban road dust pollution by heavy metal(loid)s exposed to desert dust storms in a rapid-growing city of Iran. *Environ. Earth Sci.* **82**, 316. https://doi.org/10.1007/s12665-023-11000-3 (2023).

4. Dytłow, S. & Górka-Kostrubiec, B. Concentration of heavy metals in street dust: an implication of using different geochemical background data in estimating the level of heavy metal pollution. *Environ. Geochem. Health.* **43**, 521–535. https://doi.org/10.1007/s10653-020-00726-9 (2021).

5. Mohammadpour, A., Abbasi, F., Gili, M. R., Kazemi, A. & Bell, M. L. Evaluation of concentration and characterization of potential toxic elements and fluorine in ambient air dust from Iran's industrial capital: a health risk assessment using Monte Carlo simulation. *Int. J. Appl. Earth Obs Geoinfor.* **132**, 103998. https://doi.org/10.1016/j.jag.2024.103998 (2024).

6. Guo, B. et al. Ecological risk evaluation and source apportionment of heavy metals in park playgrounds: a case study in Xi'an, Shaanxi Province, a northwest city of China. *Environ. Sci. Pollut Res.* **27**, 24400–24412. https://doi.org/10.1007/s11356-020-08744-x (2020).

7. Zhang, Z., Yang, X., Simay, Z. & Mohammed, A. Health risk evaluation of heavy metals in green land soils from urban parks in Urumqi, northwest China. *Environ. Sci. Pollut Res.* **25**, 4459–4473. https://doi.org/10.1007/s11356-017-0737-0 (2018).

8. Han, X., Lu, X., Wu, Y. & Qinggeletu. & Health risks and contamination levels of heavy metals in dusts from parks and squares of an industrial city in semi-arid area of China. *Int. J. Environ. Res. Public. Health.* **14**, 886. https://doi.org/10.3390/ijerph14080886 (2017).

9. Huang, C. C. et al. A comprehensive approach to quantify the source identification and human health risk assessment of toxic elements in park dust. *Environ. Geochem. Health.* **45**, 5813–5827. https://doi.org/10.1007/s10653-023-01588-7 (2023).

10. Siddiqui, Z., Khillare, P. S., Jyethi, D. S., Aithani, D. & Yadav, A. K. Pollution characteristics and human health risk from trace metals in roadside soil and road dust around major urban parks in Delhi city. *Air Qual. Atmos. Health.* **13**, 1271–1286. https://doi.org/10.1007/s11869-020-00874-y (2020).

11. Verma, A. & Yadav, S. Chemical speciation, bioavailability and human health risk assessment of metals in surface dust from an industrial cluster in India. *Arch. Environ. Contam. Toxicol.* **84**, 267–283. https://doi.org/10.1007/s00244-023-00984-5 (2023).

12. Niu, S., Song, X., Yu, J., Wang, X. & Lian, J. Particle size dependent heavy metals in road dusts from Maanshan City, China. *KSCE J. Civ. Eng.* **24**, 1411–1423. https://doi.org/10.1007/s12205-020-2193-5 (2020).

13. Han, Q. et al. Health risk assessment and bioaccessibilities of heavy metals for children in soil and dust from urban parks and schools of Jiaozuo, China. *Ecotoxicol. Environ. Saf.* **191**, 110157. https://doi.org/10.1016/j.ecoenv.2019.110157 (2020).

14. Mohammed, S. & Mohammed, F. K. Pollution characteristics, risk assessment, and source apportionment of potentially toxic elements in road dust at two industrial parks in Trinidad and Tobago, West Indies. *Environ. Monit. Assess.* **194**, 445. https://doi.org/10.1007/s10661-022-10109-5 (2022).

15. Jooybari, S. A., Peyrowan, H., Rezaee, P. & Gholami, H. Evaluation of pollution indices, health hazards and source identification of heavy metal in dust particles and storm trajectory simulation using HYSPLIT model (case study: Hendijan center dust, southwest of Iran). *Environ. Monit. Assess.* **194**, 107. https://doi.org/10.1007/s10661-022-09760-9 (2022).

16. Ransome, G. & Mohammed, F. K. An assessment of heavy metals in dust at recreational parks in Trinidad, West Indies: contamination status, source identification and health risk implications. *Chem. Pap.* **77**, 7067–7083. https://doi.org/10.1007/s11696-023-02999-7 (2023).

17. Kicińska, A. & Bożęcki, P. Metals and mineral phases of dusts collected in different urban parks of Krakow and their impact on the health of city residents. *Environ. Geochem. Health.* **40**, 473–488. https://doi.org/10.1007/s10653-017-9934-5 (2018).

18. Du, Y. et al. Health risk assessment of heavy metals in road dusts in urban parks of Beijing, China. *Procedia Environ. Sci.* **18**, 299–309. https://doi.org/10.1016/j.proenv.2013.04.039 (2013).

19. Wang, J. et al. Bioaccessibility, sources and health risk assessment of trace metals in urban park dust in Nanjing, Southeast China. *Ecotoxicol. Environ. Saf.* **128**, 161–170. https://doi.org/10.1016/j.ecoenv.2016.02.020 (2016).

20. Li, J. et al. Contamination, ecological-health risks, and sources of potentially toxic elements in road-dust sediments and soils of the largest urban riverfront scenic park in China. *Environ. Geochem. Health.* **45**, 8169–8186. https://doi.org/10.1007/s10653-023-01715-4 (2023).

21. Liu, Q., Wang, Y., Liu, J., Wang, Q. & Zou, M. Grain-size distribution and heavy metal contamination of road dusts in urban parks and squares in Changchun, China. *Environ. Geochem. Health.* **37**, 71–82. https://doi.org/10.1007/s10653-014-9631-6 (2015).

22. Kyene, M. O. et al. Bioaccessibility and children health risk assessment of soil-laden heavy metals from school playground and public parks in Accra, Ghana. *Environ. Monit. Assess.* **195**, 1199. https://doi.org/10.1007/s10661-023-11818-1 (2023).

23. Zhang, Y. et al. Hydrochemistry appraisal, quality assessment and health risk evaluation of shallow groundwater in the Mianyang area of Sichuan Basin, southwestern China. *Environ. Earth Sci.* **80**, 576. https://doi.org/10.1007/s12665-021-09894-y (2021).

24. Zhao, C., Zhou, B. & Su, X. Evaluation of urban eco-security—a case study of Mianyang city, China. *Sustain.* **6**, 2281–2299. https://doi.org/10.3390/su6042281 (2014).

25. Du, H. & Lu, X. Spatial distribution and source apportionment of heavy metal(loid)s in urban topsoil in Mianyang, Southwest China. *Sci. Rep.* **12**, 10407. https://doi.org/10.1038/s41598-022-14695-9 (2022).

26. Du, H., Lu, X. & Han, X. Spatial distribution characteristics and source apportionment of heavy metal(loid)s in park dust in the Mianyang urban area, China. *Environ. Geochem. Health.* **46**, 104. https://doi.org/10.1007/s10653-024-01901-y (2024).

27. MBS (Mianyang Bureau of Statistics). Mianyang statistical yearbook. (2023). http://tjj.my.gov.cn/tjnj/index.html. (Accessed: 8th March 2024).

28. Zhuang, S., Lu, X., Yu, B., Fan, X. & Yang, Y. Ascertaining the pollution, ecological risk and source of metal(loid)s in the upstream sediment of Danjiang River, China. *Ecol. Indic.* **125**, 107502. https://doi.org/10.1016/j.ecolind.2021.107502 (2021).

29. Pan, H., Lu, X. & Lei, K. Contamination identification of trace metals in roadway dust of a typical mountainous county in the Three Gorges Reservoir region, China, and its relationships with socio-economic factors. *Sustain.* **12**, 5624. https://doi.org/10.3390/su12145624 (2020).

30. Huang, J. et al. Health risk assessment of heavy metal(loid)s in park soils of the largest megacity in China by using Monte Carlo simulation coupled with positive matrix factorization model. *J. Hazard. Mater.* **415**, 125629. https://doi.org/10.1016/j.jhazmat.2021.125629 (2021).

31. Yang, Y. et al. Source-specific risk judgement and environmental impact of potentially toxic elements in fine road dust from an integrated industrial city, North China. *J. Hazard. Mater.* **458**, 131982. https://doi.org/10.1016/j.jhazmat.2023.131982 (2023).

32. Cui, Y., Bai, L., Li, C., He, Z. & Liu, X. Assessment of heavy metal contamination levels and health risks in environmental media in the northeast region. *Sustain. Cities Soc.* **80**, 103796. https://doi.org/10.1016/j.scs.2022.103796 (2022).

33. Bai, L., Li, C., Yu, C. W. & He, Z. Air pollution and health risk assessment in northeastern China: a case study of Jilin Province. *Indoor Built Environ.* **30** (10), 1857–1874. https://doi.org/10.1177/1420326X20979274 (2021).

34. Li, C., Bai, L., He, Z. & Wang, Y. Health risk assessment of heavy metals and poly-aromatic hydrocarbons in particulate matter adsorbed by indoor air purifiers. *Indoor Built Environ.* **31** (6), 1594–1612. https://doi.org/10.1177/1420326X211052239 (2022).

35. Li, C. et al. Study on metal elements in indoor particulate matter: a case study of rural residential environment in Northeast China. *Environ. Geochem. Health.* **45**, 4867–4881. https://doi.org/10.1007/s10653-023-01543-6 (2023).

36. Li, C., Bai, L., Wang, H. & Li, Z. Promoting the design of future urban metro systems to improve air pollution: based on metal element pollution in Chinese metro system. *Sustain. Cities Soc.* **97**, 104753. https://doi.org/10.1016/j.scs.2023.104753 (2023).

37. Mohammadpour, A., Emadi, Z., Berizi, E. & Kazemi, A. Trihalomethanes in chlorinated drinking water: seasonal variations and health risk assessment in southern Iran. *Groundw. Sustain. Dev.* **27**, 101342. https://doi.org/10.1016/j.gsd.2024.101342 (2024).
38. USEPA (United States Environmental Protection Agency). *Supplemental Guidance for Developing soil Screening Level for Superfund Sites. OSWER 9355.4–24* (Office of Emergency and Remedial Response, 2002).
39. MEPPRC (Ministry of Environmental Protection of the People's Republic of China). Technical guidelines for risk assessment of soil contamination of land for construction. *(China) no HJ.* **25**, 3–2019 (2019).
40. USEPA (United States Environmental Protection Agency). *Soil Screening Guidance: Technical Background Document. EPA/540/R95/128* (Office of Solid Waste and Emergency Response, 1996).
41. Zhao, X. & Duan, X. *Highlights of the Chinese Exposure Factors Handbook (Adults)* (China Environmental Science, 2014).
42. Van den Berg, R. *Human exposure to soil contamination: a qualitative and quantitative analysis towards proposals for human toxicological intervention values.* National Institute of Public Health and Environmental Protection (RIVM), Bilthoven, the Netherlands. Report no. 725201011 (1995).
43. Mohammadpour, A. et al. The concentration of potentially toxic elements (PTEs) in drinking water from Shiraz, Iran: a health risk assessment of samples. *Environ. Sci. Poll. Res.* **30**, 23295–23311. https://doi.org/10.1007/s11356-022-23535-2 (2023).
44. Mohammadpour, A., Motamed-Jahromi, M., Moreno–Jimenez, E., Golaki, M. & Berizi, E. Novel modelling approach to assess elements contamination in drinking water from Southern Iran. *Expo Health.* **16**, 661–678. https://doi.org/10.1007/s12403-023-00584-7 (2024).
45. Mohammadpour, A., Keshtkar, M., Samaei, M. R., Isazadeh, S. & Khaneghah, A. M. Assessing water quality index and health risk using deterministic and probabilistic approaches in Darab County, Iran; a machine learning for fluoride prediction. *Chemosphere.* **352**, 141284. https://doi.org/10.1016/j.chemosphere.2024.141284 (2024).
46. Afsharian, Z. et al. The concentrations and health risks of potassium sorbate and sodium benzoate in some Iranian food products: a Monte Carlo simulation. *J. Food Comp. Anal.* **135**, 106640. https://doi.org/10.1016/j.jfca.2024.106640 (2024).
47. Gupta, S. & Gupta, S. K. Application of Monte Carlo simulation for carcinogenic and non-carcinogenic risks assessment through multi-exposure pathways of heavy metals of river water and sediment, India. *Environ. Geochem. Health.* **45**, 3465–3486. https://doi.org/10.1007/s10653-022-01421-7 (2023).
48. CNEMC (China National Environmental Monitoring Centre). *The Background Values of Elements in Chinese Soils* (Environmental Science Press of China, 1990).
49. Wang, H., Shen, C., Kang, Y., Deng, Q. & Lin, X. Spatial distribution of pollution characteristics and human health risk assessment of exposure to heavy elements in road dust from different functional areas of Zhengzhou, China. *Environ. Sci. Pollut Res.* **27**, 26650–26667. https://doi.org/10.1007/s11356-020-08942-7 (2020).
50. Li, H. H. et al. Pollution characteristics and risk assessment of human exposure to oral bioaccessibility of heavy metals via urban street dusts from different functional areas in Chengdu, China. *Sci. Total Environ.* **586**, 1076–1084. https://doi.org/10.1016/j.scitotenv.2017.02.092 (2017).
51. Lam, K. C., Ng, S. L., Hui, W. C. & Chan, P. K. Environmental quality of urban parks and open spaces in Hong Kong. *Environ. Monit. Assess.* **111**, 55–73. https://doi.org/10.1007/s10661-005-8039-2 (2005).
52. Wang, Q., Lu, X. & Pan, H. Analysis of heavy metals in the re-suspended road dusts from different functional areas in Xi'an, China. *Environ. Sci. Pollut Res.* **23**, 19838–19846. https://doi.org/10.1007/s11356-016-7200-5 (2016).
53. Zhang, M. & Wang, H. Concentrations and chemical forms of potentially toxic metals in road-deposited sediments from different zones of Hangzhou, China. *J. Environ. Sci.* **21**, 625–631. https://doi.org/10.1016/s1001-0742(08)62317-7 (2009).
54. Chen, X., Ward, T. J., Sarkar, C., Ho, K. F. & Webster, C. Health risks of adults in Hong Kong related to inhalation of particle bound heavy metal(loid)s. *Air Qual. Atmos. Health.* **15**, 691–706. https://doi.org/10.1007/s11869-021-01115-6 (2022).

## Acknowledgements

## Author contributions

X.L. designed the study, conducted data analysis and the paper revision. H.D. and X.H. performed the sample collection and the experiment. H.D. designed tables and graphs, and the paper writing. All authors reviewed the manuscript.

## Declarations

### Competing interests

The authors declare no competing interests.
**Correspondence** and requests for materials should be addressed to X. L.

### Additional information

**Supplementary Information** The online version contains supplementary material available at https://doi.org/10.1038/s41598-024-79157-w.

**Correspondence** and requests for materials should be addressed to X.L.

**Reprints and permissions information** is available at www.nature.com/reprints.

**Publisher's note** Springer Nature remains neutral with regard to jurisdictional claims in published maps and institutional affiliations.